



**AALBORG UNIVERSITY**  
DENMARK

**Aalborg Universitet**

## **Toxic effects of substituted p-benzoquinones and hydroquinones in in vitro bioassays are altered by reactions with the cell assay medium**

Tentscher, Peter R.; Escher, Beate I.; Schlichting, Rita; König, Maria; Bramaz, Nadine; Schirmer, Kristin; von Gunten, Urs

*Published in:*  
Water Research

*DOI (link to publication from Publisher):*  
[10.1016/j.watres.2021.117415](https://doi.org/10.1016/j.watres.2021.117415)

*Creative Commons License*  
CC BY 4.0

*Publication date:*  
2021

*Document Version*  
Publisher's PDF, also known as Version of record

[Link to publication from Aalborg University](#)

*Citation for published version (APA):*

Tentscher, P. R., Escher, B. I., Schlichting, R., König, M., Bramaz, N., Schirmer, K., & von Gunten, U. (2021). Toxic effects of substituted p-benzoquinones and hydroquinones in in vitro bioassays are altered by reactions with the cell assay medium. *Water Research*, 202, Article 117415. <https://doi.org/10.1016/j.watres.2021.117415>

### **General rights**

Copyright and moral rights for the publications made accessible in the public portal are retained by the authors and/or other copyright owners and it is a condition of accessing publications that users recognise and abide by the legal requirements associated with these rights.

- Users may download and print one copy of any publication from the public portal for the purpose of private study or research.
- You may not further distribute the material or use it for any profit-making activity or commercial gain
- You may freely distribute the URL identifying the publication in the public portal -

### **Take down policy**

If you believe that this document breaches copyright please contact us at [vbn@aub.aau.dk](mailto:vbn@aub.aau.dk) providing details, and we will remove access to the work immediately and investigate your claim.



## Toxic effects of substituted *p*-benzoquinones and hydroquinones in *in vitro* bioassays are altered by reactions with the cell assay medium

Peter R. Tentscher<sup>a,b,1</sup>, Beate I. Escher<sup>c,d</sup>, Rita Schlichting<sup>c</sup>, Maria König<sup>c</sup>, Nadine Bramaz<sup>a</sup>, Kristin Schirmer<sup>a,e,f</sup>, Urs von Gunten<sup>a,f,\*</sup>

<sup>a</sup> Eawag, Swiss Federal Institute of Aquatic Science and Technology, Duebendorf CH-8600, Switzerland

<sup>b</sup> Department of Chemistry and Bioscience, Aalborg University, Aalborg 9220, Denmark

<sup>c</sup> Department of Cell Toxicology, UFZ – Helmholtz Centre for Environmental Research, Leipzig 04318, Germany

<sup>d</sup> Center for Applied Geoscience, Eberhard Karls University of Tübingen, Schnarrenbergstr. 94-96, Tübingen 72076, Germany

<sup>e</sup> Department of Environmental Systems Science, ETH Zürich, Zürich CH-8092, Switzerland

<sup>f</sup> Civil and Environmental Engineering (ENAC), School of Architecture, École Polytechnique Fédérale de Lausanne (EPFL), Lausanne CH-1015, Switzerland

### ARTICLE INFO

#### Keywords:

Oxidative stress  
Genotoxicity  
Carcinogenicity  
Electrophiles  
Oxidation  
Quinones

### ABSTRACT

Substituted *para*-benzoquinones and hydroquinones are ubiquitous transformation products that arise during oxidative water treatment of phenolic precursors, for example through ozonation or chlorination. The benzoquinone structural motive is associated with mutagenicity and carcinogenicity, and also with induction of the oxidative stress response through the Nrf2 pathway. For either endpoint, toxicological data for differently substituted compounds are scarce. In this study, oxidative stress response, as indicated by the AREc32 *in vitro* bioassay, was induced by differently substituted *para*-benzoquinones, but also by the corresponding hydroquinones. Bioassays that indicate defense against genotoxicity (p53RE-bla) and DNA repair activity (UmuC) were not activated by these compounds. Stability tests conducted under incubation conditions, but in the absence of cell lines, showed that tested *para*-benzoquinones reacted rapidly with constituents of the incubation medium. Compounds were abated already in phosphate buffer, but even faster in biological media, with reactions attributed to amino- and thiol-groups of peptides, proteins, and free amino acids. The products of these reactions were often the corresponding substituted hydroquinones. Conversely, differently substituted hydroquinones were quantitatively oxidized to *p*-benzoquinones over the course of the incubation. The observed induction of the oxidative stress response was attributed to hydroquinones that are presumably oxidized to benzoquinones inside the cells. Despite the instability of the tested compounds in the incubation medium, the AREc32 *in vitro* bioassay could be used as an unspecific sum parameter to detect *para*-benzoquinones and hydroquinones in oxidatively treated waters.

### 1. Introduction

Oxidative treatment steps are applied in both drinking water and wastewater treatment, with the goal of disinfection and/or the abatement of organic micropollutants (Lee and von Gunten, 2010; von Gunten, 2018). The most commonly applied oxidants in water treatment are chlorine and ozone (von Gunten, 2018). Chlorine and Chloramine are among the cheapest and most widely applied chemicals for drinking water disinfection (Deborde and von Gunten, 2008; Sedlak and von Gunten, 2011), but are also used for wastewater disinfection, either before discharge into surface waters, or in the context of water reuse

(Winward et al., 2008). Ozone (O<sub>3</sub>) has been applied as a disinfectant/oxidant for drinking water treatment for the last 100 years (von Gunten and von Sonntag, 2012), and ozonation has been recently considered and implemented for the abatement of organic micropollutants in secondary wastewater effluents (Bourgin et al., 2018; Hollender et al., 2009; Huber et al., 2005; Lee et al., 2013, 2014).

Oxidants react with different compounds in solution, including biomolecules, dissolved organic matter, or xenobiotic organic compounds such as pesticides, pharmaceuticals and personal care products. These reactions do not lead to a mineralization of the targeted or non-targeted reaction partners but yield oxidized transformation products (Deborde

\* Corresponding author.

E-mail address: [urs.vongunten@eawag.ch](mailto:urs.vongunten@eawag.ch) (U. von Gunten).

<sup>1</sup> Present address: Federal Institute for Occupational Safety and Health, Dortmund, Germany.

and von Gunten, 2008; Lee and von Gunten, 2010; Plewa and Richardson, 2017; Richardson 2017). The latter may be a health concern, as the treated waters are used for drinking water or may affect the ecosystem health in receiving freshwater bodies. In this context, it is unlikely that new compounds are formed that exhibit specific modes of toxicity such as estrogenicity or antibiotic activity. On the contrary, such specific effects are usually removed from the treated waters upon oxidation (Huber et al., 2004; Lee et al., 2008). However, one concern is the formation of electrophiles, reactive chemicals that could eventually act in a genotoxic and consequently carcinogenic manner.

Our recent study on the ozonation of phenolic compounds showed that (substituted) electrophilic *p*-benzoquinones (*p*-BQs) should be ubiquitous ozonation transformation products of phenolic precursor compounds, arising from both organic micropollutants and dissolved organic matter (DOM) (Tentscher et al., 2018). Other products of the reactions of ozone with phenols are catechols,  $\alpha,\beta$ -unsaturated ketones, and to some extent also (substituted) hydroquinones (HQs). Chlorination of drinking water supplies typically yields chlorinated compounds that are of toxicological concern, such as halomethanes or haloacetic acids (Richardson et al., 2007). A recently discovered class of electrophilic disinfection byproducts are halobenzoquinones and  $\alpha,\beta$ -unsaturated C4-dicarbonyl ring cleavage products (Diana et al., 2019; Du et al., 2013; Hung et al., 2019; Prasse et al., 2020). Also halobenzoquinones were found to be formed from phenolic precursor compounds (Wane et al., 2015).

As the precursors for these types of transformation products are structurally diverse, the formation of an equally diverse mix of substituted *p*-BQs, HQs, catechols and other  $\alpha,\beta$ -unsaturated dienones can be expected from ozonation and chlorination. These compound classes have been generally recognized as cytotoxic as well as mutagenic or carcinogenic (Benigni and Bossa, 2011; Monks et al., 1992; O'Brien, 1991).

No clear relationship between structure and mutagenicity or carcinogenicity can be observed: Mutagenicity of *p*-BQs has been found in different *Salmonella* strains, and carcinogenicity data is scarce (Table S2). Some HQs and catechols, other possible transformation products of phenol ozonation, were previously found to be weak carcinogens (Table S3). However, other compounds in these classes did not trigger such toxicological responses.

Both 1,2-*ortho*- and 1,4-*para*-quinones are listed as carcinogenic structural alerts (SA) by Benigni and Bossa (2011). This classification is based on the ISSCAN database, which lists Ames mutagenicity and rodent carcinogenicity data for 11 *p*-anthraquinones, 2 *p*-naphthoquinones, and 3 *p*-BQs (unsubstituted BQ (BQ), mitomycin-C, and trenimon, all contained in Table S2). The SA is thus based chiefly on anthraquinone data, and its generality is not clear.

Along with other halogenated disinfection byproducts, halogenated *p*-BQs are suspected to cause bladder cancer (Diana et al., 2019). Dichloro- and dibromobenzoquinone were shown to induce the oxidative stress response through the Nrf2 pathway, as well as tumor suppression activity (Li et al., 2018; Prochazka et al., 2015), and thus oxidative stress might be a cause for the possible carcinogenicity of these compounds. Also unsubstituted *p*-BQ is known to induce the Nrf2 pathway, as are some diphenols (Tables S2 and S3).

The detection of potentially mutagenic *p*-BQs in treated water by chemical analyses is complicated by the structural diversity of this class of compounds. As an alternative, a sum parameter directly related to toxic effects, such as *in vitro* bioassays, is more promising. The AREc32 (Wang et al., 2006) and Nrf2-CALUX (van der Linden et al., 2014) bioassays can be used to evaluate the toxicity of drinking water disinfection byproducts (Stalter et al., 2016). These rather general tests rely on the cell's antioxidant response (Nrf2 pathway) to oxidants that could eventually lead to mutagenic effects, but also to any indirect activation of oxidative stress response. Even though this response seems quite promising for oxidative water treatment, the change in Nrf2 response upon ozonation of wastewater has not been explicitly studied so far

(Volker et al., 2019).

Nrf2 is activated by oxidation of Keap1 or electrophilic attack/addition on Keap1, which leads to dissolution of the Keap1-Nrf2 complex. Once free, Nrf2 migrates to the nucleus to induce the antioxidant response element (ARE) that triggers the formation of cytoprotective enzymes. In the AREc32 assay, a reporter gene is coupled to the ARE that expresses luciferase, which can be detected photometrically.

Two mechanisms are possible for the toxic effects of *p*-BQs (O'Brien, 1991): (1) Arylation of e.g., peptides or DNA (direct induction of toxicity) and (2) formation of reactive oxygen species (ROS) through autooxidation and redox cycling (indirect induction of toxicity). Both arylation of Keap1 (Abiko and Kumagai, 2013; Dunlap et al., 2012; Wang et al., 2010) and oxidation of Keap1 through ROS such as H<sub>2</sub>O<sub>2</sub> can activate the Nrf2 (Covas et al., 2013; Erlank et al., 2011; Fourquet et al., 2010). Some structurally simple *p*-BQs have been shown to activate Nrf2 (Table S2) (Abiko and Kumagai, 2013; Abiko et al., 2011; Erlank et al., 2011; Rubio et al., 2011). From general chemical considerations, *p*-BQs are  $\alpha,\beta$ -unsaturated ketones, a structural motive known to react with nucleophiles through Michael-addition. Addition reactions of unsubstituted BQ have been shown for amines, thiols, and related biomolecules such as amino acids and proteins (Morrison et al., 1969), e.g., albumin in blood serum (Ghosh et al., 2012), cytochrome (Fisher et al., 2007), human topoisomerase II $\alpha$  (Bender et al., 2007), or DNA nucleobases (Gaskell et al., 2004; Xie et al., 2005).

The result of these reductive addition reactions are substituted HQs (Urano et al., 1994), also found for less electrophilic compounds such as *t*-butyl-*p*-BQ. HQs can be oxidized to *p*-BQs, and undergo further addition reactions, e.g., a BQ-monothioether can still bind to cytochrome (Person et al., 2005). Under oxic conditions, autooxidation of HQs and subsequent additions to the resulting *p*-BQs leads to increasingly substituted *p*-BQs/HQs. In the case of glutathione (GSH) as a nucleophile, eventually four GSH molecules can be added to one BQ (Baigi et al., 2008).

HQs are not electrophilic *per se*. However, structurally simple diphenols (HQs and catechols) (Dinkova-Kostova and Wang, 2011; Erlank et al., 2011; Rubio et al., 2011) or complex (Marjan et al., 2021; Na and Surh, 2008; Patel and Maru, 2013) polyphenols that contain diphenolic moieties are also known to activate the Nrf2 pathway (Table S3). Considering that diphenols such as HQ can auto-oxidize to *p*-BQs, the observed toxicity could be ascribed to *p*-BQs formed *in situ*. The finding that oxidation of differently substituted HQs by Cu(II) (Wang et al., 2010) enhances the Nrf2-AREc32 activity supports this argument. Both HQ and catechol were found to bind to guanine and thymine in the presence of Cu(II), attributed to their oxidation to the corresponding *p/o*-BQs (Hirakawa et al., 2002). Also DNA adducts from dosed HQs have been found (Tozlovanu et al., 2006) and were attributed to addition after auto-oxidation of HQs. Other studies found similar ARE-LUC (a bioassay also testing the Nrf2 pathway) activity for HQ and BQ in human bronchial epithelial cells (Rubio et al., 2011), a result that might be explained by oxidation of dosed HQs to *p*-BQs.

A second, indirect toxic mode of action is constituted by ROS, such as H<sub>2</sub>O<sub>2</sub> and superoxide radical anion. These can be formed from redox processes involving *p*-BQs and HQs as a redox couple (also possible for *o*-BQ/catechol) and can in turn induce an oxidative stress response. The autooxidation of HQs to *p*-BQs yields H<sub>2</sub>O<sub>2</sub> as a ROS. Futile redox cycling through reduction by the two-electron quinone oxidoreductase NQO1 can transform quinones to their diphenolic form (shown for menadione) (Ross et al., 2000), or through the reaction with ascorbate (Morrison et al., 1969), which reduces *p*-BQs back to their HQ forms, leading to more H<sub>2</sub>O<sub>2</sub> upon re-oxidation. Semiquinone radicals (HO-Ph-O<sup>•</sup>) can be formed through the con-proportionation of a HQ/*p*-BQ redox couple (HQ + *p*-BQ  $\rightleftharpoons$  2 HO-Ph-O<sup>•</sup>) (Eyer, 1991), or through an enzymatic one-electron reduction of a *p*-BQ (O'Brien, 1991), and the radical can reduce molecular oxygen to superoxide radical anion as an additional ROS.

Concurrent modes of action are possible (direct and indirect

induction of toxicity), as shown for menadione (a naphthoquinone), that causes cytotoxicity through both arylation and redox cycling (Chung et al., 1999; Seung et al., 1998). Cytotoxicity was found to increase when menadione was allowed to react with plasma proteins in the incubation medium, which was attributed to more efficient redox cycling of the conjugated species, and prompted the development of a medium-free protocol (Seung et al., 1998).

There is little data on the toxic potency and reactivity of differently substituted HQs and *p*-BQs. Here, a variety of commercially available model compounds comprising both *p*-BQs and HQs were tested for the response of the AREc32 bioassay. This is a rather unspecific test for oxidative stress, probing the activation of the Nrf2 pathway, which can be an initial cause for carcinogenicity (Robertson et al., 2020). For selected compounds, we also tested for effects that are more closely related to eventual carcinogenic effects that might follow from oxidative stress: the UmuC (DNA repair activity) and the p53RE-bla (tumor suppression) bioassays.

Since *p*-BQs are also reactive towards nucleophiles that may be

present in biological media, we investigated the abatement of *p*-BQs and HQs in different reaction media (phosphate buffered saline (PBS), amino acids, and fetal bovine serum (FBS)), mimicking incubation conditions. Such reactions may lead to products that have different toxicological properties compared to the parent compounds. It has been shown for 2,6-diCl-*p*-benzoquinone that pre-incubation in buffer or in amino acids reduces the cytotoxicity towards human colon epithelial cells and liver carcinoma cells (Hung et al., 2019), an effect attributed to the conjugation of the parent compound to molecules in the medium. For structurally diverse *p*-BQs, it is so far unclear which role such reactions play during incubation conditions of *in vitro* bioassays such as the AREc32 bioassay, and what type of reaction products are prevalent under these conditions.

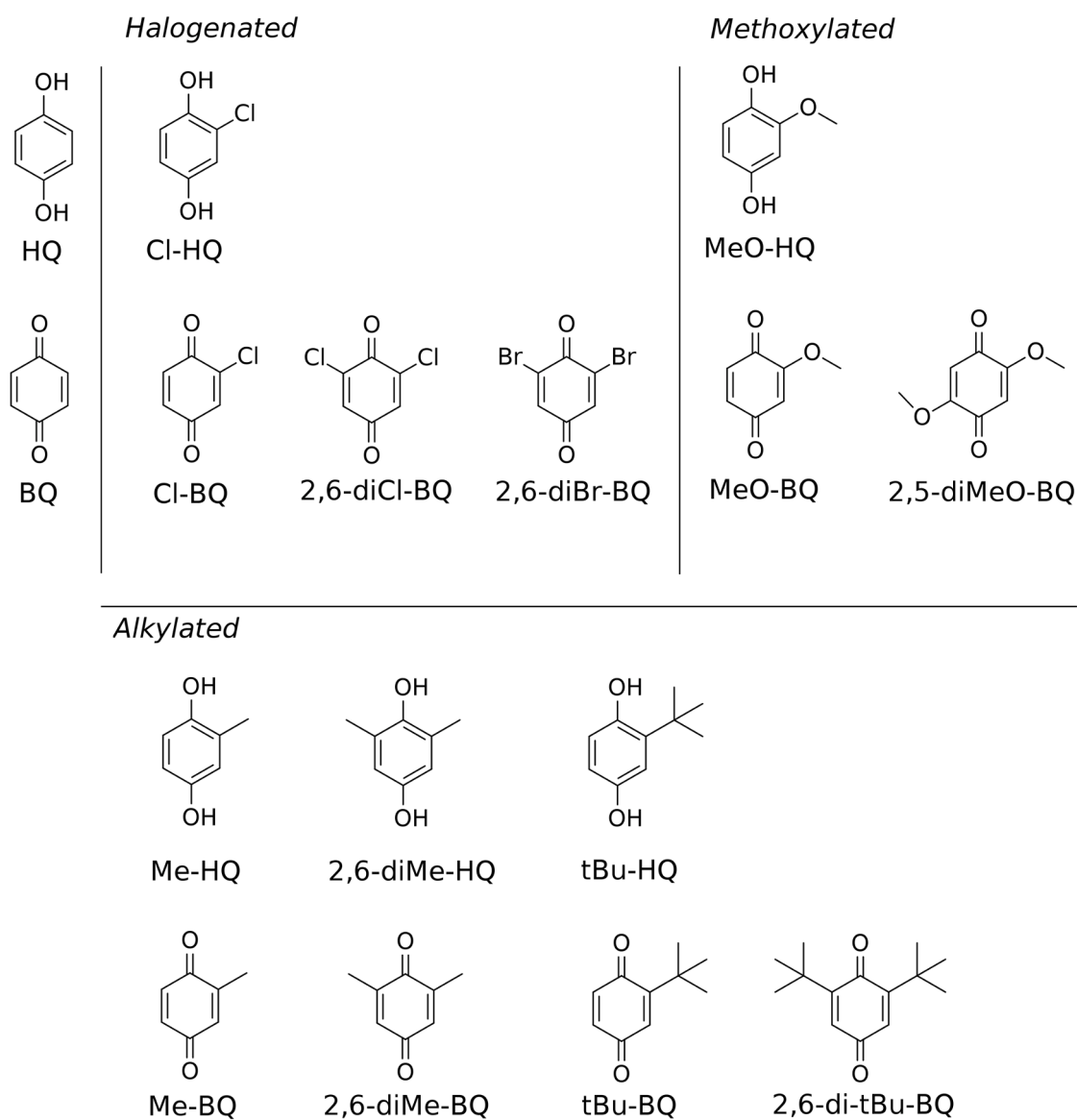


**Fig. 1.** Selected HQs and *p*-BQs used in this study: Hydroquinone (HQ), *p*-benzoquinone (BQ), chlorohydroquinone (Cl-HQ), chloro-*p*-benzoquinone (Cl-BQ), 2,6-dichloro-*p*-benzoquinone (2,6-diCl-BQ), 2,6-dibromo-*p*-benzoquinone (2,6-diBr-BQ), methoxyhydroquinone (MeO-HQ), methoxy-*p*-benzoquinone (MeO-BQ), 2,5-dimethoxy-*p*-benzoquinone (2,5-diMeO-BQ), methylhydroquinone (Me-HQ), methyl-*p*-benzoquinone (Me-BQ), 2,6-dimethylhydroquinone (2,6-diMe-HQ), 2,6-dimethyl-*p*-benzoquinone (2,6-diMe-BQ), *tert*-butyl-hydroquinone (tBu-HQ), *tert*-butyl-*p*-benzoquinone (tBu-BQ), 2,6-di-*tert*-butyl-*p*-benzoquinone (2,6-di-tBu-BQ).

## 2. Materials and methods

### 2.1. List of chemicals

A list of *p*-BQs and HQs used as test compounds in this study is provided in Fig. 1. A complete list of chemicals, suppliers and purities is given in the Supporting Information (SI), Table S1, and the physico-chemical properties are given in Table S4.

### 2.2. In vitro bioassays

#### 2.2.1. AREc32 in vitro bioassay

The AREc32 reporter cell line is based on the MCF7 breast cancer cell line with a gene encoding for luciferase attached (Wang et al., 2006) and was obtained by courtesy of C. Roland Wolf, Cancer Research UK. The AREc32 assay was performed in DMEM Glutamax with 10% FBS (standard protocol) or 1% FBS (Escher et al., 2012) brought to a 384 well plate format (Neale et al., 2017). All *p*-BQs/HQs were weighted in brown vials and stored under argon, if indicated on the packaging. On the day of the experiment, the compounds were directly dissolved in the bioassay medium to a concentration four times higher than the highest concentration in the bioassay in a so-called dosing vial that was vortexed to facilitate dissolution. The resulting compound concentration in this stock solution was  $\geq 40 \mu\text{M}$ . The preparation of the dosing vials took up to 30 min. Fourteen dosing vials were then stacked on a robot tray together with two vials of positive control (tBu-HQ) and used to prepare serial or linear dilutions in medium in a dosing plate using a pipetting robot (Hamilton Microlab Star, Bonaduz, Switzerland) that subsequently transferred 10  $\mu\text{L}$  of the dosing plate into a cell plate containing cells and 30  $\mu\text{L}$  medium using a 96-tip pipet head. The workflow of dosing is described in Escher et al. (2019a) and lasts approximately 20 to 25 min. Hence, the dosed chemicals were in contact with the medium for up to 1 h before incubation with cells started. The initial experiments using medium with 10% FBS were range finders for the activation of ARE and these experiments were only used to derive the cytotoxicity  $\text{IC}_{10}$  (inhibitory concentrations causing 10% of reduction of cell viability quantified by the Presto Blue (Thermo Fisher Scientific, A13261) according to Neale et al. (2017) because the activation of ARE proved to be too variable (data not shown). The  $\text{IC}_{50}$  were derived from a plot of logarithmic concentrations against % cell viability using a log-logistic concentration-response model Eq. (1) with the conversion from the fitted  $\text{IC}_{50}$  to  $\text{IC}_{10}$  by Eq. (2).

$$\text{Cytotoxicity (\%)} = \frac{100}{1 + 10^{(\log(\text{IC}_{50} - \text{concentration}) \times \text{slope})}} \quad (1)$$

$$\log(\text{IC}_{10}) = \log(\text{IC}_{50}) - \frac{\log(1/9)}{\text{slope}} \quad (2)$$

The main experiments were performed under stricter time control for the dosing experiment applying linear dilutions at non-cytotoxic concentrations. Two sets of experiments were run with 10% (standard conditions) and 1% FBS, each in two independent repeats. The  $\text{EC}_{\text{IR}1.5}$  is the concentration of a compound at which the induction of the reporter cell line was 50% higher than that of the unexposed cells Escher et al., 2012). The  $\text{EC}_{\text{IR}1.5}$  and its standard error  $\text{SE}(\text{EC}_{\text{IR}1.5})$  were deduced with Eqs. (3) and (4) from slopes of the linear concentration-IR (induction ratio) curves (Escher et al., 2018).

$$\text{EC}_{\text{IR}1.5} = \frac{0.5}{\text{slope}} \quad (3)$$

$$\text{SE}(\text{EC}_{\text{IR}1.5}) \approx \frac{0.5}{\text{slope}^2} \text{SE}(\text{slope}) \quad (4)$$

#### 2.2.2. p53 in vitro bioassay

The p53 bioassay was performed analogously to the AREc32 assay.

The commercially available CellSensor™ p53RE-bla HCT-116 cell-based assay developed by Invitrogen was used in this project to measure the p53 activation, according to the protocol provided by Invitrogen, with an extended incubation period of 48 h (Stalter et al., 2016). None of the tested compounds were found to induce p53 activity. The results of initial dosing experiments were used to derive cytotoxicity  $\text{IC}_{10}$  values. Since there was no activation of p53 detected, no linear repeats were run.

#### 2.2.3. UmuC/UmuC NM8001 in vitro bioassay

UmuC and UmuC NM8001 (Takamura-Enya et al., 2011) (more sensitive to oxidative DNA damage, obtained by courtesy of Prof. Yoshimitsu Oda) were tested for unsubstituted (UmuC) and also substituted (UmuC NM8001) HQs and *p*-BQs in the absence of the S9 enzyme mix. No activation was observed below cytotoxic concentrations (Text S1, SI).

### 2.3. Stability experiments in the components of the incubation medium

The incubation medium used for the AREc32 bioassay consists of Dulbecco's modified eagle medium (DMEM) and 10% fetal bovine serum (FBS), in a carbonate buffer system (pH 7.4) maintained by a  $\text{CO}_2$  atmosphere. In this medium, nucleophiles that can potentially react with *p*-BQs are  $\text{HO}^-$ , amino acids contained in DMEM, and protein-bound thiol groups in FBS. To evaluate their respective influence on *p*-BQ and HQ stability, abatement experiments were performed without reporter cell lines in PBS ( $\text{HO}^-$ ), DMEM in carbonate buffer (amino acids), and FBS buffered in PBS (thiol groups), mimicking the incubation conditions. The different approaches are sketched in Fig. 2.

After spiking *p*-BQs into PBS (Fig. 2a) or DMEM (Fig. 2b), samples were taken over the course of 24 h and stabilized by acidification. For the reactions with thiols contained in FBS, the kinetic timeframe for the abatement of three selected *p*-BQs (BQ, Me-BQ, 2,6-diMe-BQ) was established with an on-line photometric experiment (Fig. 2c). Based on these results, batch experiments were performed by adding *p*-BQs to either FBS or GSH (as a substitute source of thiols), sampled over 60 min (Fig. 2d). Residual concentrations of *p*-BQs and HQs were measured by HPLC-DAD. All experimental details are described in Text S2, SI. The photostability of *p*-BQs and HQs is briefly discussed in Text S5, SI.

### 2.4. Quantification of reactive sulfide groups in FBS

*p*-BQs can react with thiol groups stemming from cysteine moieties in FBS. For a meaningful comparison to GSH concentrations, the concentrations of sulfide groups in FBS were quantified photometrically. In a quartz cuvette, FBS solutions (5 and 10%) were prepared in 70 mM PBS (pH 7.4) containing 1 mM EDTA, to a final volume of 3 mL. 100  $\mu\text{L}$  of a 2 mM solution of Ellman's reagent (DTNB, 5,5'-dithiobis-(2-nitrobenzoic acid)) were spiked into the stirred cuvette. Absorption was monitored at 412 nm, and an extinction coefficient of  $14,150 \text{ M}^{-1} \text{ cm}^{-1}$  was used to quantify  $\text{TNB}^{2-}$ , the monomeric form of DTNB, which is formed from its reaction with thiols, after subtracting a background spectrum of FBS. As the absorption at 412 nm kept increasing, time series of  $\geq 60$  min were recorded. The concentration of  $\text{TNB}^{2-}$  monomer was equated to the concentration of reactive sulfide groups in solution. Control experiments with GSH as a source of free sulfides were also performed.

### 2.5. HPLC analysis of p-BQs and HQs

BQs and HQs were quantified by HPLC-DAD (Agilent 1100) using external standards. The compounds were separated with two different setups, (1) on a Cosmosil 5C18-MS-II (3.0  $\times$  100 mm, 5  $\mu\text{m}$ ) HPLC column at 30 °C with a flux of 600  $\mu\text{L}/\text{min}$ , and (2) on a Cosmosil 5C18-MS-II (3.0  $\times$  150 mm, 5  $\mu\text{m}$ ) at 30 °C with a flux of 800  $\mu\text{L}/\text{min}$ . Depending on the analytes, isocratic conditions (10% MeOH, 90%  $\text{H}_2\text{O}$  or 90% 0.1%  $\text{H}_3\text{PO}_4$ ) were maintained for up to 4 min, then the MeOH



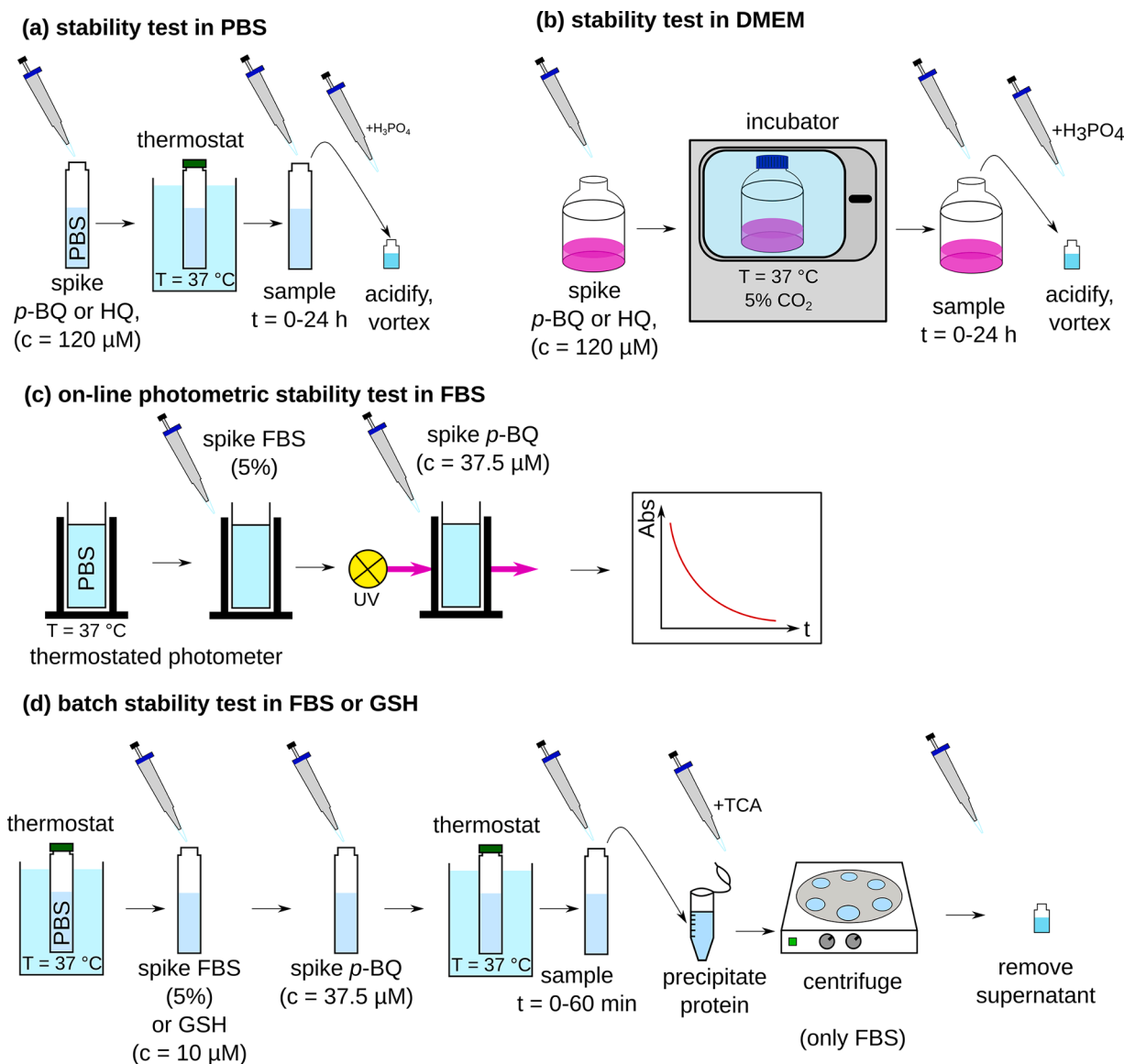


**Fig. 2.** Protocols to assess the stability of para-benzoquinones ( $p$ -BQs) and hydroquinones (HQs) under incubation conditions (pH 7.4, 37 °C) towards (a) hydroxide in phosphate buffered saline (PBS), (b) amino acids in Dulbecco's modified eagle medium (DMEM), and (c, d) thiol groups in fetal bovine serum (FBS). For (a), (b), and (d), the final samples were analyzed by HPLC-DAD for residual concentrations of the spiked  $p$ -BQs and HQs. Abbreviations: glutathione (GSH), trichloroacetic acid (TCA).

concentration was increased to 50 or 75% within 3–5 min. Injection volumes were 40–100  $\mu\text{L}$ .

### 3. Results and discussion

#### 3.1. Stability of $p$ -BQs and HQs in medium

Limited reproducibility of AREc32 test results was observed, together with similar (cyto)toxicity for  $p$ -BQs and their corresponding HQs. Since functional groups (amine, thiol) are potentially reacting with  $p$ -BQs, this prompted us to test the stability of  $p$ -BQs and HQs in the incubation media, mimicking incubation conditions. Three degradation modes (hydrolysis (PBS), reaction with amines (DMEM), reaction with thiols (FBS, GSH)) can be proposed and were tested according to Fig. 2. An additional experiment determined the concentration of accessible/reactive thiols in FBS.

##### 3.1.1. PBS and DMEM

Concentration profiles for the selected  $p$ -BQs and HQs determined by HPLC are shown in Fig. 3. In PBS, compounds behave differently depending on substitution pattern and compound type: all HQs were readily abated, and formation of the corresponding  $p$ -BQ was observed in most cases. Conversely, alkyl- $p$ -BQs were relatively stable in PBS, whereas other  $p$ -BQs were abated over the course of hours down to few minutes (Cl-BQ), with diCl-BQ no longer detectable minutes after spiking, and diBr-BQ degrading even faster, preventing meaningful quantification (no time series shown for these compounds). For these highly unstable  $p$ -BQs, the corresponding HQs were detected (diCl-BQ) or presumed (diBr-BQ, based on HPLC retention time and optical spectrum) products of these reactions.

In DMEM, HQs were abated similarly as in PBS. However, there was less formation of corresponding  $p$ -BQs as a product. The reason for this can be seen in the concentration profiles when  $p$ -BQs were spiked: the abatement of  $p$ -BQs in DMEM was more rapid compared to PBS, and some of them mostly degraded in the first minutes of incubation. In

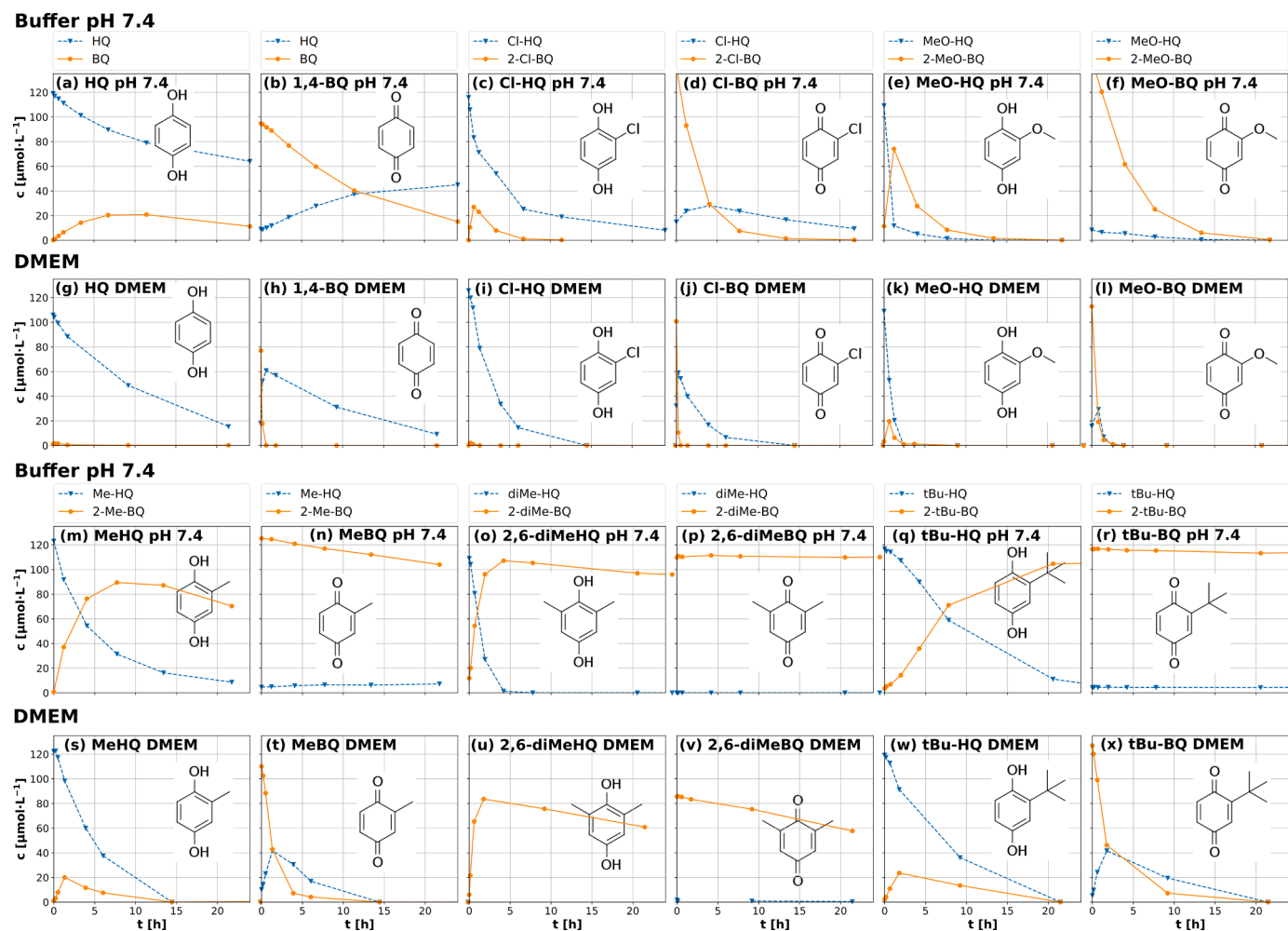
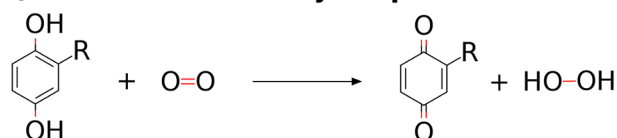
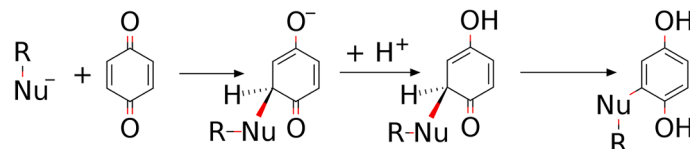


Fig. 3. Evolution of the concentrations of HQs and *p*-BQs spiked into (a–f, m–r) PBS (pH 7.4) and (g–l, s–x) DMEM, at 37 °C. Structures shown in each subplot refer to the dosed compound. The respective corresponding compound (e.g., HQ for dosed BQ or BQ for dosed HQ, respectively) was quantified as well.

**(a) Autooxidation of hydroquinones**



**(b) Reductive addition to benzoquinones**



**(c) Redox cross-reactions between hydroquinones and benzoquinones**

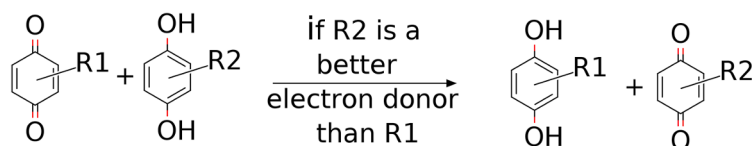


Fig. 4. Reactions of (a) HQs with ambient oxygen (b) *p*-BQs with a negatively charged nucleophile (equivalent reactions with neutral nucleophiles such as amines are also possible) and (c) *p*-BQs and HQs with each other.

contrast to PBS, alkylated *p*-BQs were readily degraded in DMEM, with the exception of 2,6-diMe-BQ.

The observed transformations of HQs and *p*-BQs can be explained by their known patterns of reactivity. Unsubstituted HQ can auto-oxidize to form BQ and H<sub>2</sub>O<sub>2</sub> (Eyer, 1991; La Mer and Rideal, 1924; Monks et al., 1992; Song and Buettner, 2010), shown in Fig. 4a. This reaction is pH-dependent, and in the presence of BQ, it proceeds through a semi-quinone radical anion pathway (Eyer, 1991; Song and Buettner, 2010), leading to overall complex kinetics. For holding times of 24 h, the substituted HQs were generally consumed to 100%, and only the unsubstituted HQ remained at about 50% (Fig. 3a). The product of these reactions is the corresponding *p*-BQ, which is stable in buffer only in some cases as discussed below.

*p*-BQs are electrophilic  $\alpha,\beta$ -unsaturated carbonyl compounds, which are susceptible to Michael-addition of nucleophiles to the C=C bond. This reductive addition yields a HQ with the nucleophile as an additional substituent (Fig. 4b). Pairs of HQs and *p*-BQs (but also catechols and the corresponding 1,2-benzoquinones) can undergo redox-cross reactions to reach a thermodynamically more stable redox state (Fig. 4c) (Uchimiya and Stone, 2006).

A reductive addition to a *p*-BQ can always be followed by a redox cross-reaction: the resulting substituted HQ is more electron-rich than the HQ that bears the same substituents as the parent *p*-BQ. Consequently, it is thermodynamically favorable to oxidize the substituted HQ to a substituted *p*-BQ, and in turn to reduce a parent *p*-BQ to a correspondingly substituted HQ (Fig. 5). The expected stoichiometry for these reactions is that for each parent *p*-BQ reacting with a nucleophile, an additional *p*-BQ is reduced to a HQ. Hence two parent *p*-BQ molecules react to one additionally substituted *p*-BQ and one HQ with the same substitution pattern as the parent, i.e., the yield of each of the two products is 0.5 in terms of consumed *p*-BQ.

The different tested solutions (PBS, DMEM, FBS) contain nucleophiles of different strength in different concentrations. In phosphate buffer, the only considerable nucleophile is HO<sup>-</sup>. We interpret that this species is responsible for the abatement of *p*-BQs in phosphate-buffered solutions (reductive hydrolysis). For the unsubstituted compounds, some kinetic details are known at room temperature, such as the second order rate constant of the initial attack of the hydroxide ion to *p*-BQ (Eigen and Matthies, 1961), and the second order rate constant of the redox cross-reaction between the resulting trihydroxybenzene anion and *p*-BQ (Uchimiya and Stone, 2006; von Sonntag et al., 2004). From the known kinetic data at room temperature (and omitting the resulting hydroxybenzoquinone as a nucleophile), we can estimate the half-life of

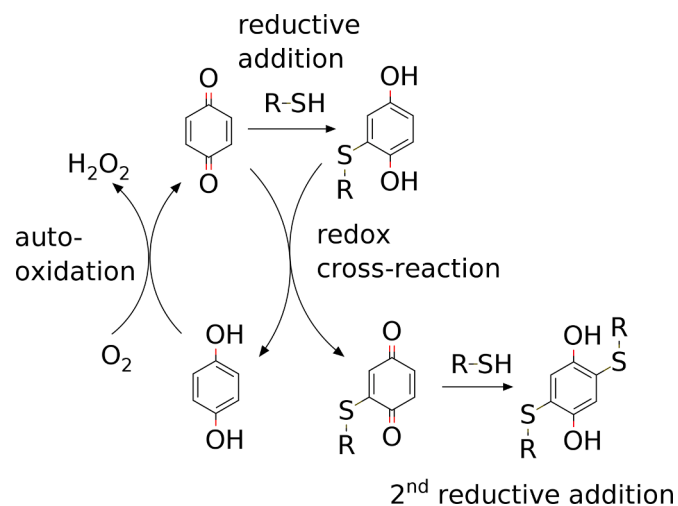


Fig. 5. Overall mechanism combining auto-oxidation of HQs, reductive addition to *p*-BQs, and redox cross-reactions between HQs and *p*-BQs, using thiol as an example of a nucleophile.

unsubstituted BQ at pH 7.4 to be 7 days. This reaction appears to be greatly accelerated at 37 °C to a half-life of about 10 h (Fig. 3b).

A higher reactivity of a *p*-BQ with electron withdrawing substituents can be expected with a nucleophile. In contrast, alkylation should slow down reductive hydrolysis through an inductive effect (+I), but potentially also through steric hindrance. This seems to be the case for reaction with HO<sup>-</sup>, as the alkylated *p*-BQs (Me-BQ, tBu-BQ, 2,6-diMe-BQ) are at most slightly degraded over the reaction time of about 20 h (Fig. 3n,p,r). The opposite effect (faster reaction) can be expected in the presence of electron-withdrawing substituents. Cl-BQ degrades more quickly in phosphate buffer compared to unsubstituted BQ. This is even more pronounced for 2,6-diCl-BQ, which vanishes completely within minutes. Following this argument, MeO-BQ should be more stable compared to BQ, owing to a mesomeric electron donation (+M-effect) of the methoxy group, but was found less stable instead. The increased reactivity of MeO-BQ is supported by a quantum chemical analysis (Text S3).

DMEM contains high concentrations (mM range) of different amino acids. These amino groups react as nucleophiles with *p*-BQs, a reaction that is exploited (with unsubstituted BQ) as a colorimetric assay for the presence of amino groups (Benson and Spillane, 1976; Hikosaka, 1970; Moxon and Slifkin, 1972). Neutral amines are stronger nucleophiles than HO<sup>-</sup> and are able to also react with the alkylated *p*-BQs. The exception was 2,6-diMe-BQ, which was also mostly stable under these conditions, possibly owing to a stronger +I-effect or increased steric hindrance. Reductive addition to amines consumed most of the tested *p*-BQs rapidly, within few minutes to one hour. The auto-oxidation of HQs should not be affected by DMEM. The slightly faster abatement of HQs in DMEM compared to PBS can be attributed to slight variations in pH. pH measurements of DMEM taken out of the incubator yielded pH values of up to 7.6, compared to the target pH of 7.4 that was maintained in experiments employing phosphate buffer. In DMEM, the auto-oxidation of HQs did not lead to a build-up of *p*-BQs, as these are consumed rapidly by their reactions with amino groups.

### 3.1.2. Kinetic experiments in FBS

Experiments were performed with unsubstituted, mono- and dimethylated *p*-BQs to cover a wide range of reactivity in 5% FBS solution in PBS. These compounds were selected since they had lower reactivities in DMEM, with 2,6-diMe-BQ being mostly stable in DMEM. These compounds can indicate whether compounds, which are stable in DMEM can still be abated in the presence of FBS. Overall, the decrease of measured absorption was rapid (Fig. 6). After 10 min, it had decreased by ~40% (BQ), ~25% (Me-BQ) and ~15% (diMe-BQ). If the loss of absorption was directly proportional to the loss in concentration of the *p*-BQs, this would correspond to drops in concentrations between ~6 and 15  $\mu$ M, but the observation might be masked by interference of products, discussed below. Nevertheless, these experiments established a time range of the initial reactions, with some very high reactivity in the first 15 min (an instantaneous concentration drop for BQ), followed by slower reactions thereafter, both getting less important with substitution. We noted that also H<sub>2</sub>O<sub>2</sub>, a potential product of redox cycling in the presence of reporter cells, degrades in an FBS solution, with 50% degradation of a 40  $\mu$ M solution in 5% FBS in ~100 min (data not shown).

### 3.1.3. Quantification of reactive sulfides in FBS

To compare the degradation of *p*-BQs to the content of accessible sulfides in FBS solutions, FBS solutions in phosphate buffer were tested with Ellman's reagent. There were approximately 20  $\mu$ M of fast-reacting sulfide groups in a 10% FBS solution typically used for AREc32 incubation (Fig. S3). For the determination of, e.g., GSH with Ellman's reagent, the concentration of TNB<sup>2-</sup> is usually determined after a reaction time of 10 min. However, FBS contains a mix of several proteins. It can be hypothesized that the reaction kinetics are determined by the accessibility of the individual thiol groups. The cysteine units at the different proteins' surfaces react immediately, whereas those further



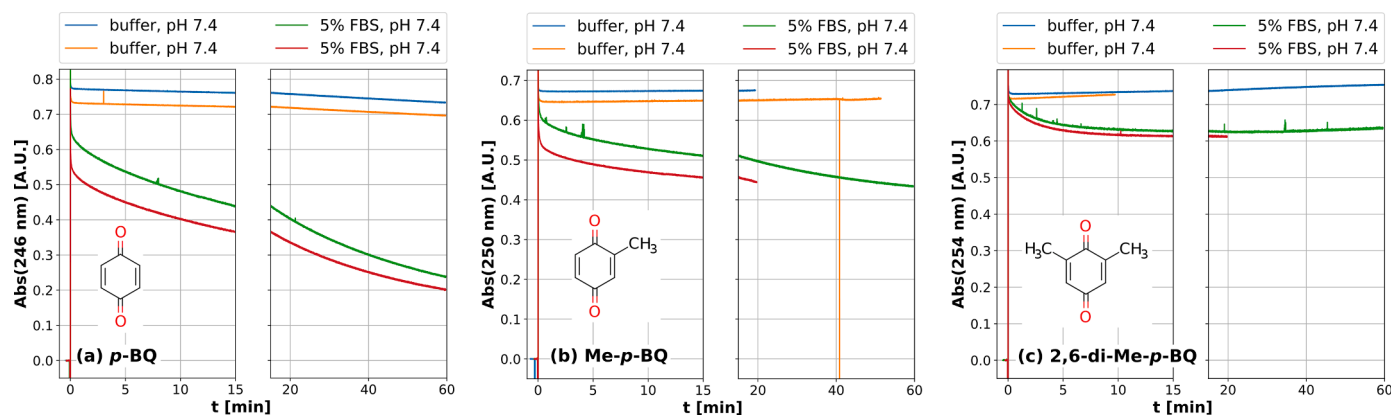


Fig. 6. Evolution of *p*-BQs spiked into a solution of 5% FBS buffered with PBS at pH 7.4 at 37 °C: (a) *para*-Benzoquinone, (b) methyl-*para*-benzoquinone, (c) 2,6-dimethyl-*para*-benzoquinone. Please note the different timescales for the left and right graphs for each compound.

inside the protein require diffusion of DTNB to these reactive sites. As DTNB is roughly twice the size of a *p*-BQ, it can be expected that benzoquinones react faster in comparison, as cysteine moieties hard to access by DTNB are reached more easily by a smaller *p*-BQ.

### 3.1.4. Batch experiments to test the abatement of *p*-BQs in presence of FBS or GSH

Batch experiments were conducted in PBS (control experiment) and in 5% FBS or in 10  $\mu$ M GSH. The results are shown as time series in Fig. 7. The abatement of *p*-BQs was clearly more rapid during the first 15 min (the first sampling point). For both FBS and GSH, HQ formation was observed. When GSH was spiked, the yield of HQ was around 0.5 mol/mol of the consumed parent *p*-BQ, while the consumption of the parent *p*-BQ was 1.7–2.0 mol/mol of added GSH (expected value of 2.0). For FBS addition, the measured HQ yields were 0.4–0.6 mol/mol of consumed parent *p*-BQ for unsubstituted *p*-BQ and Me-*p*-BQ (expected yield of 0.5). For 2,6-diMe-BQ, the HQ yield was reduced to 0.2 when measured within 24 h of the experiment. However, when the acidified samples were re-measured >30 h after the experiment, an increased HQ yield of  $\sim$ 0.4 was found.

Conversely, in the experiments conducted with a higher FBS:*p*-BQ ratio (10% FBS, 10  $\mu$ M *p*-BQ), no residual parent *p*-BQ could be detected, and only for 2,6-diMe-BQ the corresponding HQ could be detected with a molar yield of  $\sim$ 0.05. For (unsubstituted) BQ, HQ co-eluted in the HPLC with chromophoric elements of the FBS matrix, and a yield of  $\leq$   $\sim$ 0.05 could have gone undetected.

Compared to the amino acids in DMEM (e.g.,  $\sim$ 1 h to decrease the concentration of Me-BQ by 50%), these reactions are very fast (few minutes). Redox cross-reactions should also happen after the reaction of *p*-BQs with thiol groups, and lead to substituted HQs in batch experiments where an excess of *p*-BQs was dosed. However, in batch experiments where *p*-BQs were dosed under-stoichiometrically, no or only

little formation of HQs was observed. We interpret that the reductive addition to *p*-BQs kinetically outcompetes the redox cross-reaction in these cases, which is not the case for amino acids.

The continued degradation of unsubstituted BQ after 15 min (Fig. 7a) could be caused either by the reaction of BQ with the amino groups of free amino acids contained in FBS, or by continued reaction with cysteine groups that are more difficult to access but are still accessible especially to the smaller, unsubstituted BQ. The fact that the HQ yield for 2,6-diMe-BQ is initially very low likely indicates that redox cross-reactions are sterically hindered. We interpret the increase of the 2,6-diMe-HQ yield in the samples after an additional holding time as continued redox cross-reactions. A preliminary run of this experiment yielded comparable data but lacks the artefactual increase of the Me-BQ concentration in the control experiment of Fig. 7b (SI, Text S4, Fig. S4.1).

## 3.2. In vitro bioassays

Different *in vitro* bioassays were probed for their response to commercially available substituted HQs and *p*-BQs under standard incubation conditions. The main focus was on the AREc32 bioassay for oxidative stress, which was induced by almost all compounds tested. Other bioassays targeting genotoxicity (p53 GeneBLazer and UmuC/UmuC-NM8001) were not responding to the tested compounds before cytotoxic concentrations were reached.

### 3.2.1. Cytotoxicity

Inhibitory concentrations for 10% cytotoxicity (IC<sub>10</sub>) were derived from initial concentration-response experiments performed for the AREc32 and p53RE-bla bioassays (Table S5) and were found to be within  $\sim$ 10<sup>-5</sup>–10<sup>-4</sup> M for most compounds and fairly similar between the AREc32 and the p53 cell lines (Fig. 8a). The ratios of IC<sub>10</sub> of *p*-BQs

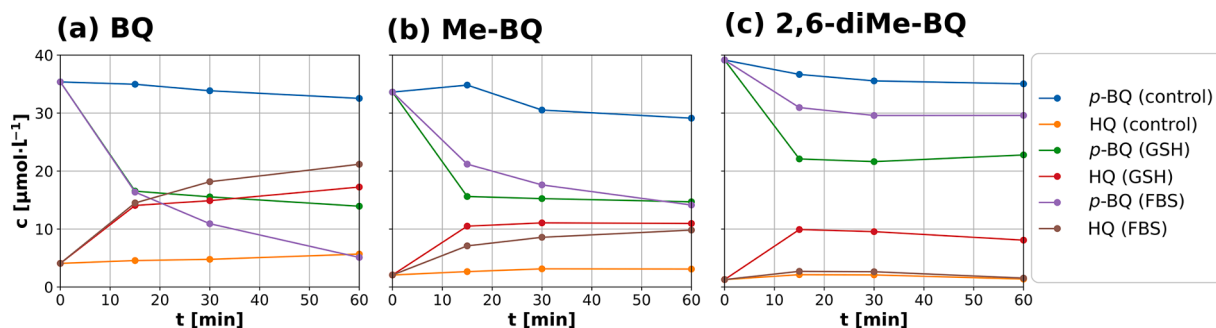
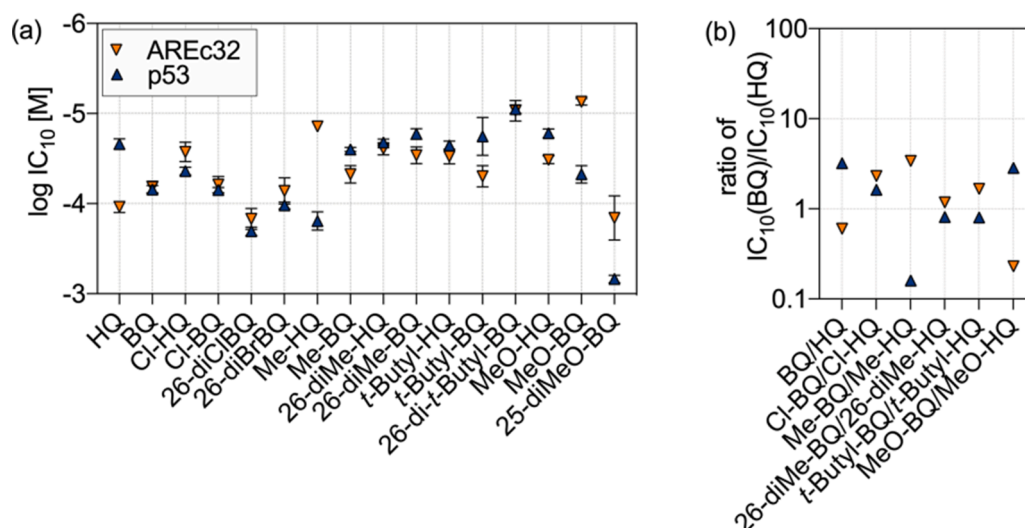


Fig. 7. Evolution of *p*-BQ and corresponding HQ concentrations at pH 7.4 at 37 °C with differently substituted *p*-BQs spiked into buffer (control), 10  $\mu$ M glutathione (GSH), and 5% FBS. (a) BQ, (b) Me-BQ, (c) 2,6-diMe-BQ.



**Fig. 8.** (a) Inhibitory concentrations for 10% cytotoxicity  $IC_{10}$  derived from AREc32 (downwards triangles) and p53RE-bla (upwards triangles) experiments. (b) Ratios of the  $IC_{10}$  triggered by *p*-BQs and HQs  $IC_{10}(BQ)/IC_{10}(HQ)$ . All  $IC_{10}$  values are provided in Table S5.

and corresponding HQs ranged from 0.23 to 3.4 for AREc32 and 0.16 to 3.2 for p53 (Fig. 8b) with the geometric mean close to 1, indicating that there are no clear sensitivity differences between the *p*-BQs and HQs.

Despite the fast degradation and loss of the parent compound, the cytotoxicity was higher than predicted by the baseline toxicity QSAR (Escher et al., 2019b) for the parent compound based on the partition constant between membrane lipids and water  $K_{lipw}$  (Fig. S4a). The excess toxicity can be described by the toxic ratio TR (Maeder et al., 2004; Verhaar et al., 1996). For MeO-BQ the TR was over 300 (Fig. S4b) and TR decreased with increasing  $K_{lipw}$  indicating that, despite degradation, the cytotoxicity was highly specific as expected for reactive chemicals (Stalter et al., 2016).

### 3.2.2. AREc32 activation

$EC_{IR1.5}$  values ranged from  $\sim 10^{-6}$  to  $\sim 3 \times 10^{-5}$  M (Fig. 9a, Table S5), and a number of chemicals (tBu-BQ, 2,6-di-tBu-BQ, MeO-HQ) did not show any activity in the range finders up to  $IC_{10}$  and were therefore not tested in the linear concentration response curve. The reproducibility of experiments was not as good as for more stable compounds that we have tested in other projects or environmental samples (Escher et al., 2013). The low repeatability of the presently investigated HQs and *p*-BQs is most likely not caused by the performance of the bioassay, but rather by some variability in the time required for sample preparation and dosing. This hypothesis is supported by the high reproducibility that

was achieved for tBu-HQ, which is regularly used as reference compound in the AREc32 reporter cell line. It was always diluted as the last sample just before starting the automated preparation of the dose response curves, followed by the transfer of the dilutions to the cell plate. Therefore, the holding time was the shortest in this case. From previous experiments, we know that the  $EC_{IR1.5}$  for tBu-HQ is much more variable if the handling of tBu-HQ during sample preparation is varied. In the present study, the  $EC_{IR1.5}$  of tBu-HQ was 1.56  $\mu$ M and in 40 independent experiments over two years, the  $EC_{IR1.5}$  varied between 1.27 and 3.43  $\mu$ M with a mean of 2.22 and a coefficient of variation of 30%.

Since  $H_2O_2$  is formed during autoxidation of HQs to *p*-BQ, we also determined the  $EC_{IR1.5}$  of  $H_2O_2$ , which was  $0.24 \pm 0.02$  mM in presence of 10% FBS and  $0.27 \pm 0.03$  mM in presence of 1% FBS.

### 3.3. Impacts of reactions with the medium on the activation of AREc32

The likely route of activation of the AREc32 bioassay by (substituted) *p*-BQs is the reaction with a thiol group of the Keap1 protein that activates the Nrf2 pathway. In turn, HQs are not electrophilic but are electron-rich compounds and should not react as electrophiles and should thus not directly induce the AREc32 assay. Since we showed that in experiments mimicking incubation conditions, HQs are quantitatively oxidized to *p*-BQs, and since HQs have been previously reported to auto-

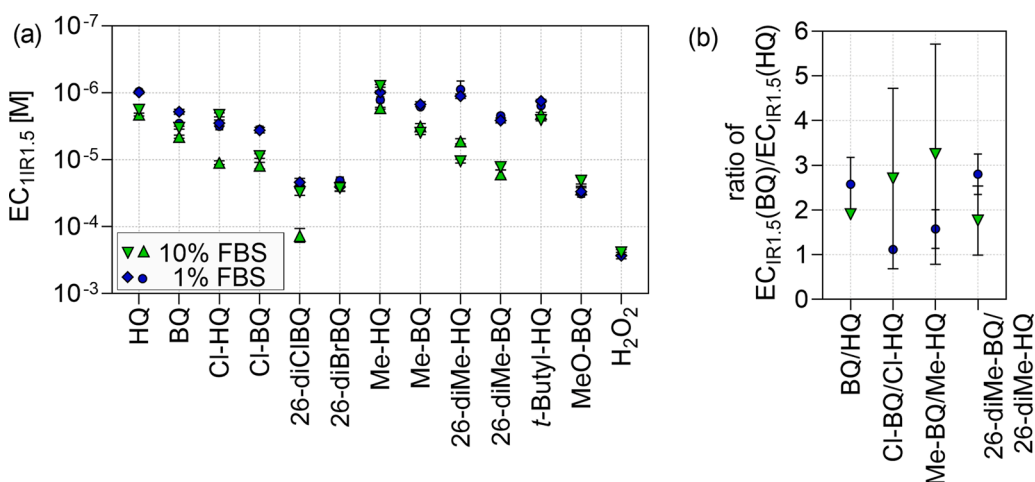


**Fig. 9.** (a)  $EC_{IR1.5}$  of different pairs of HQs and *p*-BQs from two independent experiments run with medium supplemented with 1% FBS (blue symbols, circles and diamonds) and 10% FBS (green symbols, upward and downward triangles). (b) Ratio of  $EC_{IR1.5}$  values obtained from HQs and correspondingly substituted *p*-BQs for 1% FBS (green triangles) and 10% FBS (blue circles) (For interpretation of the references to color in this figure legend, the reader is referred to the web version of this article).

oxidize to *p*-BQs and H<sub>2</sub>O<sub>2</sub> (Eyer, 1991; La Mer and Rideal, 1924; Monks et al., 1992; Song and Buettner, 2010), both *p*-BQs and H<sub>2</sub>O<sub>2</sub> could be responsible for the observed AREc32 activation.

Conversely, we showed that in 10% FBS, dosed *p*-BQs were rapidly consumed, and the same has to be expected for *p*-BQs formed *in situ* from auto-oxidation of HQs. When the dosed *p*-BQs were initially diluted in the dosing vials containing 10% FBS, compounds ( $\geq 40 \mu\text{M}$ ) are in excess of thiol groups ( $\sim 20\text{--}30 \mu\text{M}$ ). A fast reaction leading to conjugated HQs and parent HQs with a yield of up to 0.5 has to be expected. In 1% FBS, *p*-BQs are in large excess of thiol groups in the dosing vial, and the main sink are (slower) reactions with free amino acids. The timescale of these reactions depended strongly on the compound (Fig. 3, Fig. 7). However, these reactions will continue to produce HQs with a yield of  $\sim 0.5$  as the dilution procedure and the incubation progresses.

These HQs, with or without -S-R (or -NH-R) substitution, can enter the reporter cells. However, it should be considered that binding to a voluminous protein may prevent passing the cell membrane. For more hydrophobic neutral and charged chemicals, uptake kinetics into AREc32 were previously found to depend on the FBS concentration, and completed for neutral chemicals within 4 h, and were slower for charged organic molecules (Fischer et al., 2018). While AREc32 has very little constitutively expressed *CYP1A1* and accordingly no P450 CYP1 activity, *CYP1A1* can be activated by chemical exposure as has been shown with benzo[a]pyrene (Fischer et al., 2020). We showed that during the first 1 and 2 h of the incubation, most HQs are quantitatively auto-oxidized to the corresponding *p*-BQs (Fig. 3). As the timescales of auto-oxidation and cellular uptake are similar, we propose that a fraction HQs could enter the cells unchanged and could be (auto-)oxidized there, whereas another fraction undergoes extracellular auto-oxidation. This should be followed by a rapid, quantitative reaction with thiol groups of FBS, which are in large excess when a final dilution around the EC<sub>IR1.5</sub> concentration is reached in 10% FBS. No redox cross-reactions are expected in this case.

Fig. 9b shows that the ratio of EC<sub>IR1.5</sub> (BQ)/ EC<sub>IR1.5</sub> (HQ) was around 1.5–2.5 for four HQ/*p*-BQ pairs, that is, the dosed HQs induced a stronger antioxidant response because they had a lower EC<sub>IR1.5</sub>. This is compatible with the above interpretation that *p*-BQs resulting from oxidation inside the cell are ultimately responsible for the toxic effects: dosed *p*-BQs are rapidly consumed to yield either HQs at a lower concentration, or additionally substituted *p*-BQs or HQs. In contrast, dosed HQs auto-oxidize on a slower time scale (compared to the reaction of *p*-BQs with the medium) and can diffuse into the cells without prior reaction with the incubation medium. Intracellular HQs can then auto-oxidize or be transformed to *p*-BQs and can activate the Nrf2 pathway by arylation or react with other intracellular nucleophiles such as GSH.

In a scenario where a *p*-BQ was dosed and underwent reductive addition with the formation of a substituted HQ, the parent HQ yield is maximally 0.5, and thus the concentration of toxicologically active compound is reduced. Also substituted HQs that result from the reductive addition of thiols or amines to parent *p*-BQs can be oxidized to substituted *p*-BQs. Owing to the electron-donating nature of the -S-R and -NH-R substituents, these should be less electrophilic compared to the parent *p*-BQs. Both effects offer an explanation as to why HQs yield lower EC<sub>IR1.5</sub>, although these effects were only minor.

When comparing experiments in 10% FBS to 1% FBS, we can consider that these contain  $\sim 20 \mu\text{M}$  and  $\sim 2 \mu\text{M}$  of fast-reacting -SH groups, respectively. The effect of FBS content on EC<sub>IR1.5</sub> concentrations was most pronounced for 2,6-diMe-BQ/2,6-diMe-HQ (Fig. 9), the only tested compound that was mostly stable in DMEM. While all other *p*-BQs were also abated by amino acids, 2,6-diMe-BQ reacted only with -SH groups in FBS. In experiments with 1% FBS, a larger fraction of 2,6-diMe-BQ can enter the cell before undergoing reductive addition and react with the thiol group of Keap1.

### 3.4. Validity of bioassay results and implications for the toxicity of BQs and HQs

Our interpretation of the degradation experiments is that using the standard incubation condition (10% FBS), only HQs are stable enough to enter the reporter cells and are (auto)oxidized inside the cell on a timescale of few hours. The AREc32 activation experienced when dosing HQs is thus that of corresponding *p*-BQs. It is tempting to integrate over the HQ degradation to arrive at an effective exposure of the reporter cells to the *p*-BQs. However, as the *p*-BQs resulting from auto-oxidation (outside and inside the cells) or enzymatic oxidation (inside the cells) should be consumed rapidly, it is unclear how the actual exposure (concentration  $\times$  time) to these chemicals should be defined. In terms of toxic potency, the derived EC<sub>IR1.5</sub> for HQs could be interpreted as lower limits to the EC<sub>IR1.5</sub> values of the corresponding *p*-BQs. However, also substituted HQs (and substituted *p*-BQs through autooxidation) can contribute to the observed toxicity. In case of dosed *p*-BQs, the identity of the active molecules is less clear, as the products of reductive additions are likely the source of electrophiles.

Auto-oxidation of HQs always yields H<sub>2</sub>O<sub>2</sub> as a byproduct. 40  $\mu\text{M}$  H<sub>2</sub>O<sub>2</sub> reached 50% abatement after  $\sim 100$  min in a 5% FBS solution (data not shown), and was 1–2 orders of magnitude less potent than the tested *p*-BQs/HQs (Fig. 9a). If H<sub>2</sub>O<sub>2</sub> were responsible for the observed AREc32 activation, it would have to be produced with a yield of 10–100 mol/mol of the dosed parent compounds, which appears unlikely. For unsubstituted HQ, one could go through four stages of increasingly substituted HQs, and the molar yield of H<sub>2</sub>O<sub>2</sub> could be 5 at most, assuming that increasingly substituted *p*-BQs remain susceptible to further reductive addition. Also, if H<sub>2</sub>O<sub>2</sub> was the active species, the pronounced effect of FBS concentration on the EC<sub>IR1.5</sub> of 2,6-diMe-HQ/2,6-diMe-BQ could not be explained. The EC<sub>IR1.5</sub> of the HQ was lower by a factor of  $\sim 2$  compared to the *p*-BQ (Fig. 9b). This is compatible with the HQ, formed through reductive addition and a redox cross-reaction with a yield of 0.5, being the reactive species. In case of redox cycling as the dominant mode of action, no pronounced differences in EC<sub>IR1.5</sub> of a *p*-BQ/HQ pair should be expected.

This notion is supported by a study that reports the generation of H<sub>2</sub>O<sub>2</sub> by tBu-HQ in the growth medium (DMEM with 10% FBS) in the absence of cells (Erlank et al., 2011). Within one hour, H<sub>2</sub>O<sub>2</sub> was found to be present in about the same stoichiometry as the dosed tBu-HQ. In the presence of astrocytes, the H<sub>2</sub>O<sub>2</sub> yield in the medium was reduced to 25% of the dosed tBu-HQ concentration, which the authors attributed to detoxification mechanisms of the astrocytes.

*p*-BQs (dosed directly or created *in situ*) can also be expected to add rapidly to GSH or similar cell constituents. In contrast, H<sub>2</sub>O<sub>2</sub> formation inside the cell should cause the formation of GSSG. No increased GSSG levels were found upon the treatment with (unsubstituted) BQ in a medium-free dosing on blood cell platelets (Seung et al., 1998). For dimethylnaphthoquinone, a pure redox cyler (and thus intracellular producer of H<sub>2</sub>O<sub>2</sub>), increased GSSG levels were reported. However, *in vivo*, the xenobiotics will have to travel through biological medium, e.g., blood, cytoplasm, potentially leading to conjugates before entering a cell. Overall, the question of the importance of redox cycling in the toxic mechanisms of substituted *p*-BQs cannot be answered in a general manner based on the present data and may be compound-specific. In the case of halobenzoquinones, the reactions with amino acids may be so rapid and nonselective that only conjugated species are toxicologically relevant, and even unsubstituted *p*-BQ is degraded within minutes in DMEM, while alkylation protects the *p*-BQ to some extent. This may indicate that in many cases, conjugated *p*-BQs are the active species that were assessed by the AREc32 bioassay, as these are still capable of Michael-reactions as well as redox cycling. Invoking this argument and assuming that arylation is the toxic mechanism, the toxicity gradient BQ > Cl-BQ > diCl-BQ can be rationalized. The more electrophilic species readily react to less electrophilic monoconjugates, which then are weaker electrophiles than the parent compound.

### 3.5. Toxicity of HQs and BQs assessed by different bioassays

In addition to the AREc32 bioassay, which tests the antioxidant stress response, we also performed bioassays that should be more specific to genotoxicity and DNA damage. However, the compounds did not induce a response in the p53 bioassay or the UmuC NM8001 bioassay. In this variant of the UmuC assay (DNA repair activity), certain detoxification mechanisms have been removed, making it more sensitive to oxidative stress.

The incubation media of both the UmuC and p53 bioassays contain nucleophiles capable of reacting with *p*-BQs. The UmuC bioassay employs a casein digest (a protein mix) and tryptone (amino acids). The p53 bioassay was carried out in McCoy's 5A medium, which contains GSH as well as an FBS supplement. Although no p53 or UmuC activation was found, potential activity below cytotoxic concentrations may have been masked by reaction of *p*-BQs with the incubation medium. The situation would be similar in real water samples that are freeze-dried and resuspended in incubation medium prior to toxicological tests.

## 4. Conclusions

In oxidative water treatment, *p*-BQs and HQs are ubiquitous transformation products arising from phenolic precursors. *In vitro* bioassays are a potential tool for the detection of these compound classes in treated waters. Here, different bioassays were tested for their response to a structurally diverse set of model compounds, along with the substances' stability in typically used incubation media components.

- Out of the tested standard bioassays, only the AREc32 bioassay responded to almost all model compounds with  $EC_{IR1.5}$  around  $10^{-4}$  to  $10^{-6}$  M.
- All tested compounds were found to be unstable during standard incubation conditions of the AREc32 bioassay. This was attributed to the autooxidation of HQs to *p*-BQs, and to the reductive addition of nucleophiles (amino and thiol groups) to *p*-BQs.
- Reactions with the incubation medium lead to a structurally diverse mix of additionally substituted *p*-BQs and HQs. The observed  $EC_{IR1.5}$  values do not necessarily indicate the toxic potency of the different target substances.
- Virtually all *p*-BQs and HQs yielded high toxic ratios for cytotoxicity and  $EC_{IR1.5}$ , meaning that this bioassay still responds specifically to these compound classes. For applications in water quality, it should be kept in mind that the AREc32 bioassay is a rather general test of the oxidative stress response, and will respond to other types of compounds as well.
- Although the rapid reactions of *p*-BQs with biomolecules were observed at the elevated temperature of the bioassay incubation, these reactions are likely also happening in a biological post-filtration step, leading to an abatement of initially formed *p*-BQs.

## Declaration of Competing Interest

The authors declare that they have no known competing financial interests or personal relationships that could have appeared to influence the work reported in this paper.

## Funding sources

This study was funded by the Swiss National Science Foundation (SNF) project 200021\_157143. We gratefully acknowledge access to the platform CITEPro (Chemicals in the Terrestrial Environment Profiler) funded by the Helmholtz Association.

## Acknowledgement

We thank Samuel Derrer (Eawag) for help with sublimation and

recrystallization of substances, and Daniel Stalter for organizing and handling the UmuC NM-8001 strain.

## Supplementary materials

Supplementary material associated with this article can be found, in the online version, at doi:10.1016/j.watres.2021.117415.

## References

- Abiko, Y., Kumagai, Y., 2013. Interaction of Keap1 modified by 2-tert-Butyl-1,4-benzoquinone with GSH: evidence for S-Transarylation. *Chem. Res. Toxicol.* 26 (7), 1080–1087.
- Abiko, Y., Miura, T., Phuc, B.H., Shinkai, Y., Kumagai, Y., 2011. Participation of covalent modification of Keap1 in the activation of Nrf2 by tert-butylbenzoquinone, an electrophilic metabolite of butylated hydroxyanisole. *Toxicol. Appl. Pharmacol.* 255 (1), 32–39.
- Baigi, M.G., Brault, L., Neguesque, A., Beley, M., El Hilali, R., Gauzere, F., Bagrel, D., 2008. Apoptosis/necrosis switch in two different cancer cell lines: influence of benzoquinone- and hydrogen peroxide-induced oxidative stress intensity, and glutathione. *Toxicol. in Vitro* 22 (6), 1547–1554.
- Bender, R.P., Ham, A.J.L., Osheroff, N., 2007. Quinone-induced enhancement of DNA cleavage by human topoisomerase II alpha: adduction of cysteine residues 392 and 405. *Biochemistry* 46 (10), 2856–2864.
- Benigni, R., Bossa, C., 2011. Mechanisms of chemical carcinogenicity and mutagenicity: a review with implications for predictive toxicology. *Chem. Rev.* 111 (4), 2507–2536.
- Benson, G.A., Spillane, W.J., 1976. Spectrophotometric microdetermination of amines and sulfamates with 1,4-benzoquinone. *Anal. Chem.* 48 (14), 2149–2152.
- Bourgin, M., Beck, B., Boehler, M., Borowska, E., Fleiner, J., Salhi, E., Teichler, R., von Gunten, U., Siegrist, H., McArdell, C.S., 2018. Evaluation of a full-scale wastewater treatment plant upgraded with ozonation and biological post-treatments: abatement of micropollutants, formation of transformation products and oxidation by-products. *Water Res.* 129, 486–498.
- Chung, S.H., Chung, S.M., Lee, J.Y., Kim, S.R., Park, K.S., Chung, J.H., 1999. The biological significance of non-enzymatic reaction of menadione with plasma thiols: enhancement of menadione-induced cytotoxicity to platelets by the presence of blood plasma. *FEBS Lett.* 449 (2-3), 235–240.
- Covas, G., Marinho, H.S., Cyrne, L. and Antunes, F. (2013) Activation of Nrf2 by H2O2: de novo synthesis versus nuclear translocation. *Hydrogen peroxide and cell signaling*, Pt C 528, 157-171.
- Deborde, M., von Gunten, U., 2008. Reactions of chlorine with inorganic and organic compounds during water treatment - kinetics and mechanisms: a critical review. *Water Res.* 42 (1-2), 13–51.
- Diana, M., Felipe-Sotelo, M., Bond, T., 2019. Disinfection byproducts potentially responsible for the association between chlorinated drinking water and bladder cancer: a review. *Water Res.* 162, 492–504.
- Dinkova-Kostova, A.T., Wang, X.J., 2011. Induction of the Keap1/Nrf2/ARE pathway by oxidizable diphenols. *Chem. Biol. Interact.* 192 (1-2), 101–106.
- Du, H.Y., Li, J.H., Moe, B., McGuigan, C.F., Shen, S.W., Li, X.F., 2013. Cytotoxicity and oxidative damage induced by halobenzoquinones to T<sub>24</sub> bladder cancer cells. *Environ. Sci. Technol.* 47 (6), 2823–2830.
- Dunlap, T., Piyankarage, S.C., Wijewickrama, G.T., Abdul-Hay, S., Vanni, M., Litosh, V., Luo, J., Thatcher, G.R.J., 2012. Quinone-induced activation of Keap1/Nrf2 signaling by aspirin prodrugs masquerading as nitric oxide. *Chem. Res. Toxicol.* 25 (12), 2725–2736.
- Eigen, M., Matthies, P., 1961. Über Kinetik und Mechanismus der Primärreaktionen der Zersetzung von Chinon in alkalischer Lösung. *Chem. Ber.* 94 (12), 3309–3317.
- Erlank, H., Elmam, A., Kohen, R., Kanner, J., 2011. Polyphenols activate Nrf2 in astrocytes via H<sub>2</sub>O<sub>2</sub>, semiquinones, and quinones. *Free Radic. Biol. Med.* 51 (12), 2319–2327.
- Escher, B.I., Dutt, M., Maylin, E., Tang, J.Y.M., Toze, S., Wolf, C.R., Lang, M., 2012. Water quality assessment using the AREc32 reporter gene assay indicative of the oxidative stress response pathway. *J. Environ. Monit.* 14 (11), 2877–2885.
- Escher, B.I., Glauch, L., König, M., Mayer, P., Schlichting, R., 2019a. Baseline toxicity and volatility cutoff in reporter gene assays used for high-throughput screening. *Chem. Res. Toxicol.* 32 (8), 1646–1655.
- Escher, B.I., Glauch, L., König, M., Mayer, P., Schlichting, R., 2019b. Baseline toxicity and volatility cutoff in reporter gene assays used for high-throughput screening. *Chem. Res. Toxicol.* 32 (8), 1646–1655.
- Escher, B.I., Neale, P.A., Villeneuve, D.L., 2018. The advantages of linear concentration-response curves for *in vitro* bioassays with environmental samples. *Environ. Toxicol. Chem.* 37 (9), 2273–2280.
- Escher, B.I., van Daele, C., Dutt, M., Tang, J.Y.M., Altenburger, R., 2013. Most oxidative stress response in water samples comes from unknown chemicals: the need for effect-based water quality trigger values. *Environ. Sci. Technol.* 47 (13), 7002–7011.
- Eyer, P., 1991. Effects of superoxide-dismutase on the autoxidation of 1,4-hydroquinone. *Chem. Biol. Interact.* 80 (2), 159–176.
- Fischer, F.C., Abele, C., Droge, S.T.J., Henneberger, L., König, M., Schlichting, R., Scholz, S., Escher, B.I., 2018. Cellular uptake kinetics of neutral and charged chemicals in *in vitro* assays measured by fluorescence microscopy. *Chem. Res. Toxicol.* 31 (8), 646–657.



- Fischer, F.C., Abele, C., Henneberger, L., Kluver, N., Konig, M., Muhlenbrink, M., Schlichting, R., Escher, B.I., 2020. Cellular metabolism in high-throughput *in vitro* reporter gene assays and implications for the quantitative *in vitro-in vivo* extrapolation. *Chem. Res. Toxicol.* 33 (7), 1770–1779.
- Fisher, A.A., Labenski, M.T., Malladi, S., Gokhale, V., Bowen, M.E., Milleron, R.S., Bratton, S.B., Monks, T.J., Lau, S.S., 2007. Quinone electrophiles selectively adduct "electrophile binding motifs" within cytochrome. *Biochemistry* 46 (39), 11090–11100.
- Fourquet, S., Guerois, R., Biard, D., Toledano, M.B., 2010. Activation of NRF2 by nitrosative agents and H<sub>2</sub>O<sub>2</sub> involves Keap1 disulfide formation. *J. Biol. Chem.* 285 (11), 8463–8471.
- Gaskell, M., McLuckie, K.I.E., Farmer, P.B., 2004. Comparison of the mutagenic activity of the benzene metabolites, hydroquinone and para-benzoquinone in the supF forward mutation assay: a role for minor DNA adducts formed from hydroquinone in benzene mutagenicity. *Mutat. Res. Fundam. Mol. Mech. Mutagen.* 554 (1–2), 387–398.
- Ghosh, A., Choudhury, A., Das, A., Chatterjee, N.S., Das, T., Chowdhury, R., Panda, K., Banerjee, R., Chatterjee, I.B., 2012. Cigarette smoke induces *p*-benzoquinone-albumin adduct in blood serum: Implications on structure and ligand binding properties. *Toxicology* 292 (2–3), 78–89.
- Hikosaka, A., 1970. The reaction of aliphatic amines with *p*-benzoquinone. The effect of the alkyl group of amines on the reaction. *Bull. Chem. Soc. Jpn.* 43 (12), 3928–3929.
- Hirakawa, K., Oikawa, S., Hiraku, Y., Hirotsawa, I., Kawanishi, S., 2002. Catechol and hydroquinone have different redox properties responsible for their differential DNA-damaging ability. *Chem. Res. Toxicol.* 15 (1), 76–82.
- Hollender, J., Zimmermann, S.G., Koepke, S., Krauss, M., McArdell, C.S., Ort, C., Singer, H., von Gunten, U., Siegrist, H., 2009. Elimination of organic micropollutants in a municipal wastewater treatment plant upgraded with a full-scale post-ozonation followed by sand filtration. *Environ. Sci. Technol.* 43 (20), 7862–7869.
- Huber, M.M., Gobel, A., Joss, A., Hermann, N., Löffler, D., McArdell, C.S., Ried, A., Siegrist, H., Ternes, T.A., von Gunten, U., 2005. Oxidation of pharmaceuticals during ozonation of municipal wastewater effluents: a pilot study. *Environ. Sci. Technol.* 39 (11), 4290–4299.
- Huber, M.M., Ternes, T.A., von Gunten, U., 2004. Removal of estrogenic activity and formation of oxidation products during ozonation of 17 alpha-ethinylestradiol. *Environ. Sci. Technol.* 38 (19), 5177–5186.
- Hung, S., Mohan, A., Reckhow, D.A., Pollitt, K.J.G., 2019. Assessment of the *in vitro* toxicity of the disinfection byproduct 2,6-dichloro-1,4-benzoquinone and its transformed derivatives. *Chemosphere* 234, 902–908.
- La Mer, V.K., Rideal, E.K., 1924. The influence of hydrogen concentration on the auto-oxidation of hydroquinone. A note on the stability of the quinhydrone electrode. *J. Am. Chem. Soc.* 45, 223–231.
- Lee, Y., Escher, B.I., Von Gunten, U., 2008. Efficient removal of estrogenic activity during oxidative treatment of waters containing steroid estrogens. *Environ. Sci. Technol.* 42 (17), 6333–6339.
- Lee, Y., Gerrity, D., Lee, M., Bogue, A.E., Salhi, E., Gamage, S., Trenholm, R.A., Wert, E. C., Snyder, S.A., von Gunten, U., 2013. Prediction of micropollutant elimination during ozonation of municipal wastewater effluents: use of kinetic and water specific information. *Environ. Sci. Technol.* 47 (11), 5872–5881.
- Lee, Y., Kovalova, L., McArdell, C.S., von Gunten, U., 2014. Prediction of micropollutant elimination during ozonation of a hospital wastewater effluent. *Water Res.* 64, 134–148.
- Lee, Y., von Gunten, U., 2010. Oxidative transformation of micropollutants during municipal wastewater treatment: comparison of kinetic aspects of selective (chlorine, chlorine dioxide, ferrate(VI), and ozone) and non-selective oxidants (hydroxyl radical). *Water Res.* 44 (2), 555–566.
- Li, J.H., Moe, B., Liu, Y.M., Li, X.F., 2018. Halobenzoquinone-induced alteration of gene expression associated with oxidative stress signaling pathways. *Environ. Sci. Technol.* 52 (11), 6576–6584.
- Marjan Talebi, Mohsen Talebi, Tahereh Farkhondeh, Gaurav Mishra, Selen Ilgin, Saeed Samarghandian, Talebi, M., Talebi, M., Farkhondeh, T., Mishra, G., Ilgin, S., Samarghandian, S. New insights into the role of the Nrf2 signaling pathway in green tea catechin applications. *Phytotherapy Research.* 2021; 35: 3078–3112. <https://doi.org/10.1002/ptr.7033>.
- Maeder, V., Escher, B.I., Scheringer, M., Hungerbühler, K., 2004. Toxic ratio as an indicator of the intrinsic toxicity in the assessment of persistent, bioaccumulative, and toxic chemicals. *Environ. Sci. Technol.* 38 (13), 3659–3666.
- Monks, T.J., Hanzlik, R.P., Cohen, G.M., Ross, D., Graham, D.G., 1992. Quinone chemistry and toxicity. *Toxicol. Appl. Pharmacol.* 112 (1), 2–16.
- Morrison, M., Steele, W., Danner, D.J., 1969. Reaction of benzoquinone with amines and proteins. *Arch. Biochem. Biophys.* 134 (2), 515. &
- Moxon, G.H., Slikin, M.A., 1972. Interaction of proline and other amino-acids with para benzoquinone. *J. Chem. Soc. Perkin Trans.* 2 (9), 1159. &
- Na, H.K., Surh, Y.J., 2008. Modulation of Nrf2-mediated antioxidant and detoxifying enzyme induction by the green tea polyphenol EGCG. *Food Chem. Toxicol.* 46 (4), 1271–1278.
- Neale, P.A., Altenburger, R., Ait-Aissa, S., Brion, F., Busch, W., Umbuzeiro, G.D., Denison, M.S., Du Pasquier, D., Hilscherova, K., Hollert, H., Morales, D.A., Novak, J., Schlichting, R., Seiler, T.B., Serra, H., Shao, Y., Tindall, A.J., Tollefsen, K.E., Williams, T.D., Escher, B.I., 2017. Development of a bioanalytical test battery for water quality monitoring: fingerprinting identified micropollutants and their contribution to effects in surface water. *Water Res.* 123, 734–750.
- O'Brien, P.J., 1991. Molecular mechanisms of quinone cytotoxicity. *Chem. Biol. Interact.* 80 (1), 1–41.
- Patel, R., Maru, G., 2013. Polymeric black tea polyphenols induce phase II enzymes via Nrf2 in mouse liver and lungs (vol 44, pg 1897, 2008). *Free Radic. Biol. Med.* 63, 399–400.
- Person, M.D., Mason, D.E., Liebler, D.C., Monks, T.J., Lau, S.S., 2005. Alkylation of cytochrome c by (glutathion-S-yl)-1,4-benzoquinone and iodoacetamide demonstrates compound-dependent site specificity. *Chem. Res. Toxicol.* 18 (1), 41–50.
- Plewa, M.J., Richardson, S.D., 2017. Disinfection by-products in drinking water, recycled water and wastewater: formation, detection, toxicity and health effects: preface. *J. Environ. Sci.* 58, 1.
- Prasse, C., von Gunten, U., Sedlak, D.L., 2020. Chlorination of phenols revisited: unexpected formation of alpha,beta-unsaturated C-4-dicarbonyl ring cleavage products. *Environ. Sci. Technol.* 54 (2), 826–834.
- Prochazka, E., Escher, B.I., Plewa, M.J., Leusch, F.D.L., 2015. *In vitro* cytotoxicity and adaptive stress responses to selected haloacetic acid and halobenzoquinone water disinfection byproducts. *Chem. Res. Toxicol.* 28 (10), 2059–2068.
- Richardson, S., 2017. Disinfection by-products and chemical contaminants in disinfected waters. *Environ. Mol. Mutagen.* 58, S42. -S42.
- Richardson, S.D., Plewa, M.J., Wagner, E.D., Schoeny, R., DeMarini, D.M., 2007. Occurrence, genotoxicity, and carcinogenicity of regulated and emerging disinfection by-products in drinking water: a review and roadmap for research. *Mutat. Res. Mutat. Res.* 636 (1–3), 178–242.
- Robertson, H., Dinkova-Kostova, A.T., Hayes, J.D., 2020. NRF2 and the ambiguous consequences of its activation during initiation and the subsequent stages of tumorigenesis. *Cancers* 12 (12).
- Ross, D., Kepa, J.K., Winski, S.L., Beall, H.D., Anwar, A., Siegel, D., 2000. NAD(P)H: quinone oxidoreductase 1 (NQO1): chemoprotection, bioactivation, gene regulation and genetic polymorphisms. *Chem. Biol. Interact.* 129 (1–2), 77–97.
- Rubio, V., Zhang, J., Valverde, M., Rojas, E., Shi, Z.Z., 2011. Essential role of Nrf2 in protection against hydroquinone- and benzoquinone-induced cytotoxicity. *Toxicol. In Vitro* 25 (2), 521–529.
- Sedlak, D.L., von Gunten, U., 2011. The Chlorine Dilemma. *Science* 331 (6013), 42–43.
- Seung, S.A., Lee, J.Y., Lee, M.Y., Park, J.S., Chung, J.H., 1998. The relative importance of oxidative stress versus arylation in the mechanism of quinone-induced cytotoxicity to platelets. *Chem. Biol. Interact.* 113 (2), 133–144.
- Song, Y., Buettner, G.R., 2010. Thermodynamic and kinetic considerations for the reaction of semiquinone radicals to form superoxide and hydrogen peroxide. *Free Radic. Biol. Med.* 49 (6), 919–962.
- Stalter, D., O'Malley, E., von Gunten, U., Escher, B.I., 2016. Fingerprinting the reactive toxicity pathways of 50 drinking water disinfection by-products. *Water Res.* 91, 19–30.
- Takamura-Enya, T., Ishii, R., Oda, Y., 2011. Evaluation of photo-genotoxicity using the umu test in strains with a high sensitivity to oxidative DNA damage. *Mutagenesis* 26 (4), 499–505.
- Tentscher, P.R., Bourgin, M., von Gunten, U., 2018. Ozonation of para-substituted phenolic compounds yields *p*-benzoquinones, other cyclic alpha,beta-unsaturated ketones, and substituted catechols. *Environ. Sci. Technol.* 52 (8), 4763–4773.
- Tozlovanu, M., Faucet-Marquis, V., Pfohl-Leschkowicz, A., Manderville, R.A., 2006. Genotoxicity of the hydroquinone metabolite of ochratoxin A: Structure-activity relationships for covalent DNA adduction. *Chem. Res. Toxicol.* 19 (9), 1241–1247.
- Uchimiya, M., Stone, A.T., 2006. Aqueous oxidation of substituted dihydroxybenzenes by substituted benzoquinones. *Environ. Sci. Technol.* 40 (11), 3515–3521.
- Urano, M., Tateyama, M., Sakai, M., Kato, T., Kikugawa, K., Kurechi, T., 1994. Effect of tert-butylhydroquinone (Tbqh) on the formation of nitrosamines in the reaction of secondary-amines with nitrite. *Jpn. J. Toxicol. Environ. Health* 40 (6), 504–512.
- van der Linden, S.C., von Bergh, A.R.M., van Vught-Lussenburg, B.M.A., Jonker, L.R.A., Teunis, M., Krul, C.A.M., van der Burg, B., 2014. Development of a panel of high-throughput reporter-gene assays to detect genotoxicity and oxidative stress. *Mutat. Res. Genet. Toxicol. Environ. Mutagen.* 760, 23–32.
- Verhaar, H.J.M., Ramos, E.U., Hermens, J.L.M., 1996. Classifying environmental pollutants. 2: separation of class 1 (baseline toxicity) and class 2 ('polar narcosis') type compounds based on chemical descriptors. *J. Chemom.* 10 (2), 149–162.
- Volker, J., Stapf, M., Miehle, U., Wagner, M., 2019. Systematic review of toxicity removal by advanced wastewater treatment technologies via ozonation and activated carbon. *Environ. Sci. Technol.* 53 (13), 7215–7233.
- von Gunten, U., 2018. Oxidation processes in water treatment: are we on track? *Environ. Sci. Technol.* 52 (9), 5062–5075.
- von Gunten, U., von Sonntag, C., 2012. *Chemistry of Ozone in Water and Wastewater Treatment*. IWA Publishing.
- von Sonntag, J., Mvula, E., Hildenbrand, K., von Sonntag, C., 2004. Photohydroxylation of 1,4-benzoquinone in aqueous solution revisited. *Chem. A Eur. J.* 10 (2), 440–451.
- Wane, W., Qian, Y.C., Jmaiff, L.K., Krasner, S.W., Hrudey, S.E., Li, X.F., 2015. Precursors of halobenzoquinones and their removal during drinking water treatment processes. *Environ. Sci. Technol.* 49 (16), 9898–9904.
- Wang, X.J., Hayes, J.D., Higgins, L.G., Wolf, C.R., Dinkova-Kostova, A.T., 2010. Activation of the NRF2 signaling pathway by copper-mediated redox cycling of para- and ortho-hydroquinones. *Chem. Biol.* 17 (1), 75–85.
- Wang, X.J., Hayes, J.D., Wolf, C.R., 2006. Generation of a stable antioxidant response element-driven reporter gene cell line and its use to show redox-dependent activation of Nrf2 by cancer chemotherapeutic agents. *Cancer Res.* 66 (22), 10983–10994.
- Winward, G.P., Avery, L.M., Stephenson, T., Jefferson, B., 2008. Chlorine disinfection of grey water for reuse: effect of organics and particles. *Water Res.* 42 (1–2), 483–491.
- Xie, Z.W., Zhang, Y.B., Guliaev, A.B., Shen, H.Y., Hang, B., Singer, B., Wang, Z.G., 2005. The *p*-benzoquinone DNA adducts derived from benzene are highly mutagenic. *DNA Repair* 4 (12), 1399–1409.